THE ARCHIVE OF MECHANICAL ENGINEERING

VOL. LV 2008 Number 4

DOI: 10.24425/ame.2008.131630

Key words: axial flow compressor stage, unsteady flow, pressure fluctuation, rotating stall

ANDRZEJ WITKOWSKI [*], *MARCIN ZIACH* [**], *MIROSŁAW MAJKUT* [***], *MICHAŁ STROZIK* [****]

EXPERIMENTAL INVESTIGATIONS OF THE FLOW PHENOMENA IN THE ROTOR BLADES OF THE AXIAL FLOW LOW SPEED COMPRESSOR STAGE AT THE UNSTABLE PART OF THE OVERALL PERFORMANCE CHARACTERISTIC

The paper presents experimental investigations of pressure fluctuations near the tip clearance region of the rotor blades of the axial-flow low-speed compressor stage in stable and unstable parts of the overall performance characteristic. In this investigation, unsteady pressure was measured with the use of high frequency pressure transducers mounted on the casing wall of rotor passage. The pressure signals and their frequency characteristics were analyzed during the steady-state processes, before the rotating stall, during the transition from the steady-state process to the rotating stall, and during a stabilized phenomenon of low-frequency rotating stall. As the operating point moves to the unstable region of flow characteristic, an inception of the rotating stall can be observed, which rotates with a speed of about 41.4% of the rotor speed. The results of this study confirm that in the low-speed axial compressor stage operating in a rotating stall regime there appears one stall cell that spreads over to adjacent rotor blade channels. As the flow rate is reduced further, the frequency of the rotating stall decreased to 34.8% of the rotor speed and the number of blade channels with the stall cell increases.

[*] *The Silesian University of Technology, ul. Konarskiego 18, 44-100 Gliwice, Poland. E-mail: andrzej.witkowski@polsl.pl*

[**] *The Silesian University of Technology, ul. Konarskiego 18, 44-100 Gliwice, Poland. E-mail: marcin.ziach@polsl.pl*

[***] *The Silesian University of Technology, ul. Konarskiego 18, 44-100 Gliwice, Poland. E-mail: miroslaw.majkut@polsl.pl*

[****] *The Silesian University of Technology, ul. Konarskiego 18, 44-100 Gliwice, Poland. E-mail: michal.strozik@polsl.pl*

NOMENCLATURE

C_z,c_t – axial and tangential components of abdolute velocity of flow,
f – frequency of pressure oscillation,
$f_{b.p.}$ – blade passing frequency,
$f_{r.s.}$ – rotating stall frequency,
N – number of sample,
p – pressure,
PS – pressure side of the blade wake,
RMS – root mean square,
SS – suction side of the blade wake,
T_z – axial component of turbulence intensity,
t – time,
T – revolution time of compressor rotor,
u_t – blade tip speed,
ϕ – flow rate coefficient (mean axial velocity divided by rotor tip speed),
Ψ – total pressure rise corresponding to rotor tip speed,
ζ_d – kinetic energy defect,

Subscripts

$(\bar{})$ – average mean,
$(')$ – fluctuating quantity.

1. Introduction

Unsteady flow phenomena, such as periodic rotating stall with non-periodic characteristics of pressure fluctuations, deteriorate the performance and stability of compressor stage causing vibration, noise and blade excitation. Thus, the mechanism of these instabilities is worth analysing in order to avoid such unsteady phenomena. Experimental research efforts aimed at detecting and analyzing stall instabilities have been reported (e.g. Inoue al.[1], Nobuyuki et al. [2]). Since the flow in the tip region of a compressor rotor has a significant effect on the compressor stage efficiency and stability, a great deal of the reported research has been conducted in order to understand flow mechanism in that region. This is described in the cited above [1,2] and Day [3], Inoue et al. [4], Maerz et al. [5] and Kim [6]. Most of the experimental data focus on unsteady pressure measurements along the axis or around the circumference of the compressor outer wall (e.g. Nishioka et al. [7], Levy and Pismenny [8], Levy et al. [9] and Lepicovsky and Braunscheidel [10]). Motivated by the papers of the previous authors (e.g. Witkowski et al. [11-13]), the authors carried out a series of experiments utilizing unsteady flow structure measured by the Triple Split Fiber Probes (TSFP) and High Frequency Pressure Transducers (HFPT) mounted on the casing wall, both at the rotor blade leading

edge, and along the blade passage, to determine the frequency and circumferential extension of the rotating stall cell. In this study, measurements and analysis of unsteady pressure field on the casing wall, and the variation of flow structure in the span direction downstream of the rotor, were conducted to understand the flow characteristics and the structure of the stall cell under the rotating stall. We can consider the short length-scale disturbance as vortices from the rotor blades, and the long length-scale disturbances as the ones directly related to the stall process. The present paper is also concerned with the ratio of rotating stall and shaft frequency and the spread of the stall cell in the circumferential direction, as they depend on points of operation. They are distinctive features of the rotating stall phenomenon, and play an important role in the prediction and analysis of the pressure fields during rotating stall.

2. Test facility and instrumentation

2.1. Test facility

The investigations were carried out on a single-stage axial-flow low-speed compressor connected to the suction side of the measuring collector (Fig. 1). Test stage consists of an inlet guide vane followed by a rotor with a hub-to-tip annulus wall diameter ratio of 0.56, with outer diameter of 1.0 m, with 16 cambered and twisted blades of British C-4 section designed for free-vortex operation, followed by a 13-vane stator row and the outflow curvilinear diffuser with throttling blades. The dimensionless parameter of the rotor overall characteristics and tested operating points are shown in Fig. 2. The details of the design of the test stage and the test facility, their performance and geometrical features are described by Witkowski et al. [13].

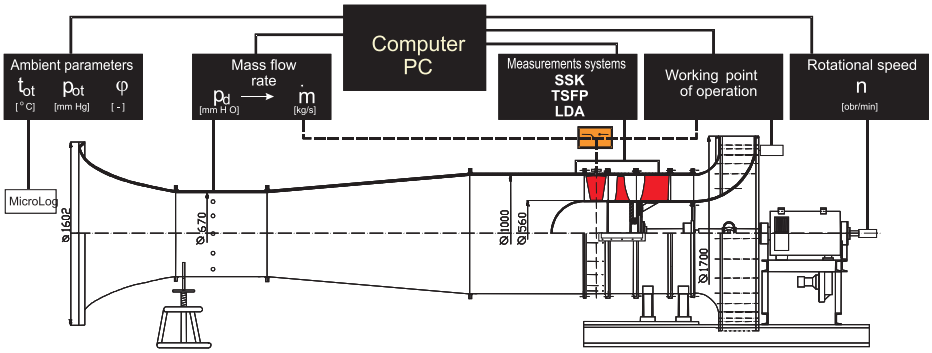

Fig. 1. Test facility and instrumentation

As the flow coefficient decreases, the pressure coefficient increases until the curve of the overall performance characteristic becomes horizontal

(Fig.2). At this time, the pressure coefficient decreases sharply. This fall continues until the flow coefficient reaches the value of 0.286. Then, the pressure coefficient increases reaching values higher than before. This three zones could be designated as "above rotating stall", "rotating stall" and "below rotating stall" (Lepicovsky and Braunscheidel [10]). The stall inception of the rotor is detected at ϕ=0.345 when the flow rate is reduced. The objective of the experimental investigations is to study in detail the flow in this low-speed axial-flow compressor stage in these three zones, in particular the unsteady but stable rotating stall structures and their variations as a function of the flow coefficient.

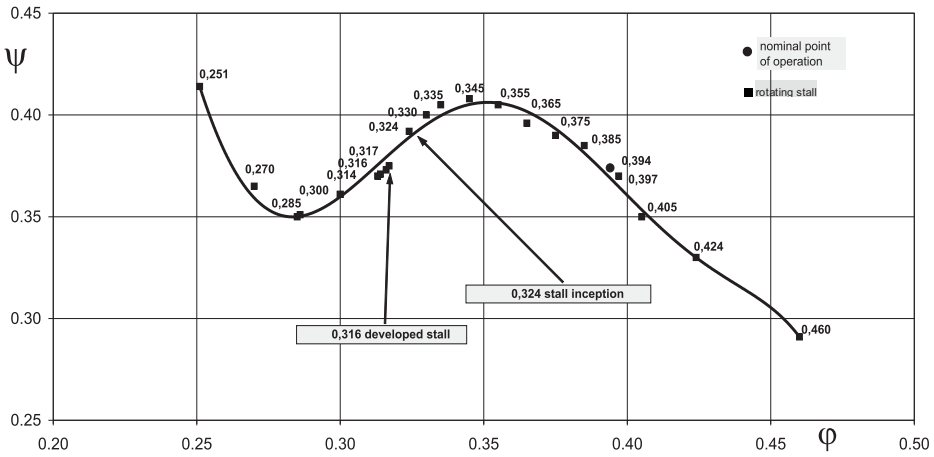

Fig. 2. Overall performance characteristic of the rotor with unsteady flow region

2.2. Instrumentation

The experimental study was conducted with the use of three measuring systems based on different principles: a five-hole pressure probe (FHPP), a fast response, straight version of the triple split fiber probe (TSFP), and high-frequency pressure transducer (HFPT). The flow field downstream of the rotor was sampled periodically using TSFP. The frequency response of this probe was 175 kHz . A more detailed description of the TSFP and its calibration procedure is given in the papers cited earlier [8,9]. The periodic multisampling and averaging technique was also employed with a high-response pressure sensor to get the phase-locked pressure distribution and its fluctuation on the casing wall. Recent advances in sensor technology allow recording a higher amount of the pressure signal data. 32 high-sensitivity pressure transducers with high natural frequency (150 kHz) were used in the experiments for measuring the unsteady pressure field on the rotor-casing wall. The circumferential location array of 16 pressure transducers, A through P, 1.3 axial

chord of the rotor ahead of the rotor leading edge, are depicted in Figure 3(a). For detailed pressure-field survey, the next 16 pressure transducers were placed along their rotor blade passage on the casing wall, as shown in Fig. 3(b).

The instantaneous pressure value was collected at the sampling rate of 0.059 ms (16.95 kHz), which corresponded to 64 circumferential sampling points between one pitch of the blade passage per one cycle. In this investigation, the phase-locked ensemble averaging technique was used for processing the measured signal.

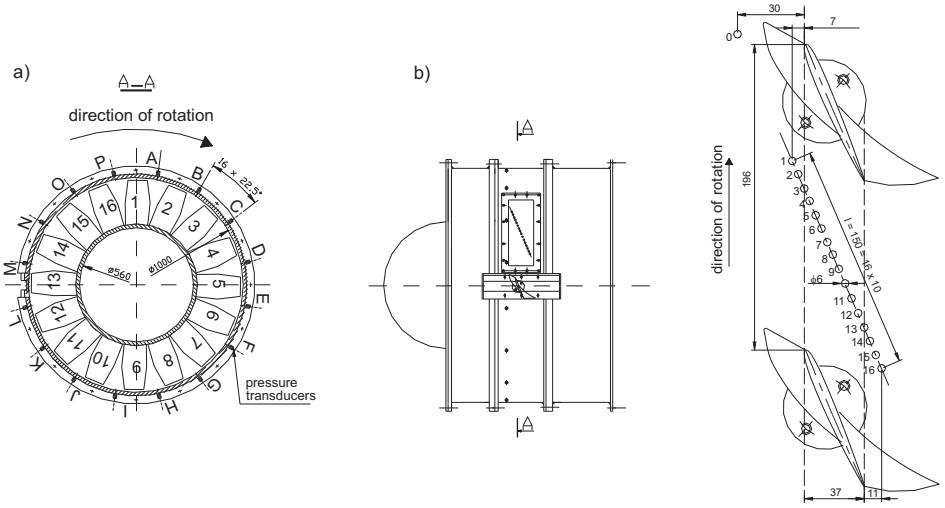

Fig. 3. Circumferential (a) and rotor blade passage (b) pressure transducer locations

3. Experimental results and discussion

3.1. Influence of point of operation on the flow characteristic

Figure 4(a) shows the variation of two mass-average axial and tangential components of velocities at various flow rates, measured along span-wise, downstream of the rotor by traversing FHPP at the measuring point, p.15 in Fig. 3(b). Fig. 4(b) indicates the RMS value of the pressure fluctuation measured using high frequency pressure transducers on the casing wall downstream of the rotor at the position (p.15). The RMS value is defined by the following equation

$$RMS = \sqrt{\frac{1}{N-1}\sum_{i=1}^{N}(p_i' - \overline{p})^2} \; ; \; \overline{p} = \frac{\sum_{i=1}^{N} p_i'}{N} \tag{1}$$

Where, p_i is instantaneous pressure value, and N number of sample.

As the flow rate decreases from ϕ=0.33 to 0.285, the tangential velocity and the RMS value significantly increase. When flow rate decreases further, the pressure is restored (Fig. 2) and the RMS value decreases. The significant effect of the flow in the tip region of compressor rotor on the compressor efficiency and stability can be estimated approximately by defining the kinetic energy defect and the turbulence intensity behind the rotor:

– kinetic energy defect

$$\zeta_d = \frac{(w_{\max})^2 - (w_n)^2}{\overline{w}^2} \tag{2}$$

where: w_n is the local ensemble average relative flow velocity and w_{max} is the outer edge velocity

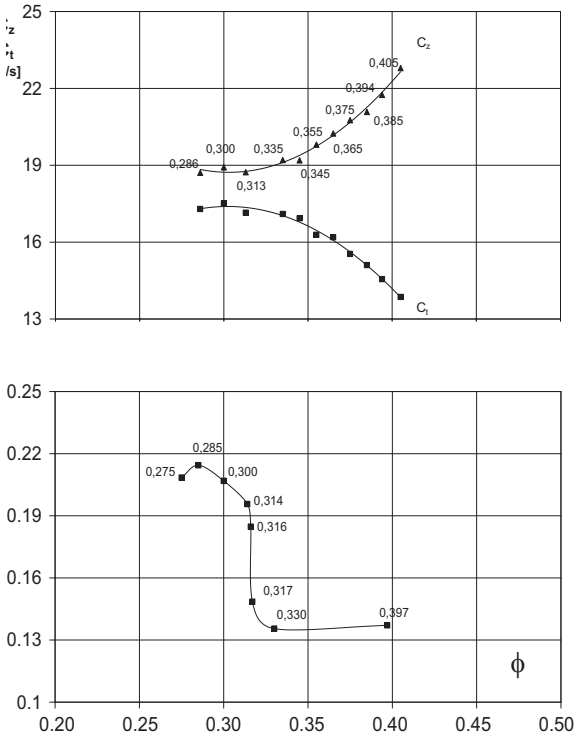

Fig. 4. (a) Mean axial and tangential components of velocities, and (b) RMS value of wall static pressure fluctuation

– axial components of the turbulence intensity

$$T_z = \sqrt{\frac{\overline{c_z'^2}}{c}} \tag{3}$$

where: $\overline{c_z'^2}$ – is the mean value of the fluctuating velocity and $\bar{c}$ mean value of the absolute velocity

The contour plots of the energy defect and turbulence intensity just downstream of the rotor blade at three flow coefficients are shown in (Figs. 5, and 6). They shows the regions of strong energy defect and highest turbulence intensity close to the hub and mainly near the outer wall. The reason for this is the accumulation of low-energy fluid near the hub and casing wall. It is also visible that the region of low-energy fluid becomes thicker at the casing and thinner at the hub in the stall condition. It is a convincing proof that the flow in the tip region of the compressor rotor has a significant effect on the compressor instability and stall inception .

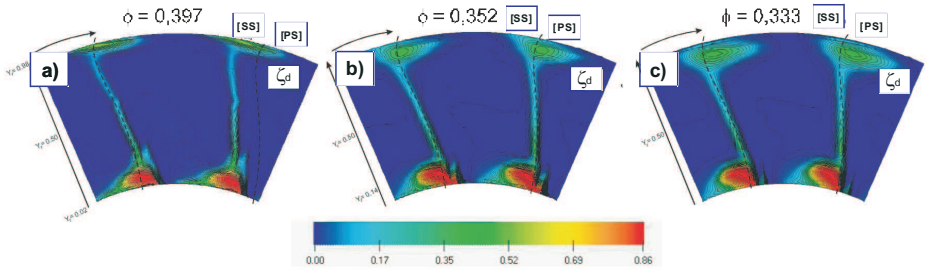

Fig. 5. Contour plots of the kinetic energy defect at different points of operation

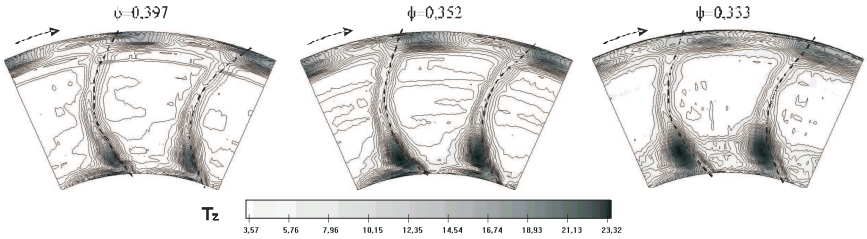

Fig. 6. Contour plots of the axial components of turbulence intensities at different points of operations

4. Unsteady pressure field in the tip region of rotor blades

4.1. Investigations of the pressure fluctuations along the rotor blade passage

Figures 7 (a,b) show a typical pressure fluctuation of the investigated compressor stage measured by pressure transducers at several axial locations along the curve corresponding to the camber of the rotor blades, as illustrated in Fig. 3b, at nominal point of operation (ϕ=0.397), and in the unsteady flow region (ϕ=0.314), respectively. The rotating instability is most clearly observed at the axial measuring station "0" in Fig. 7b, in contrast to that in

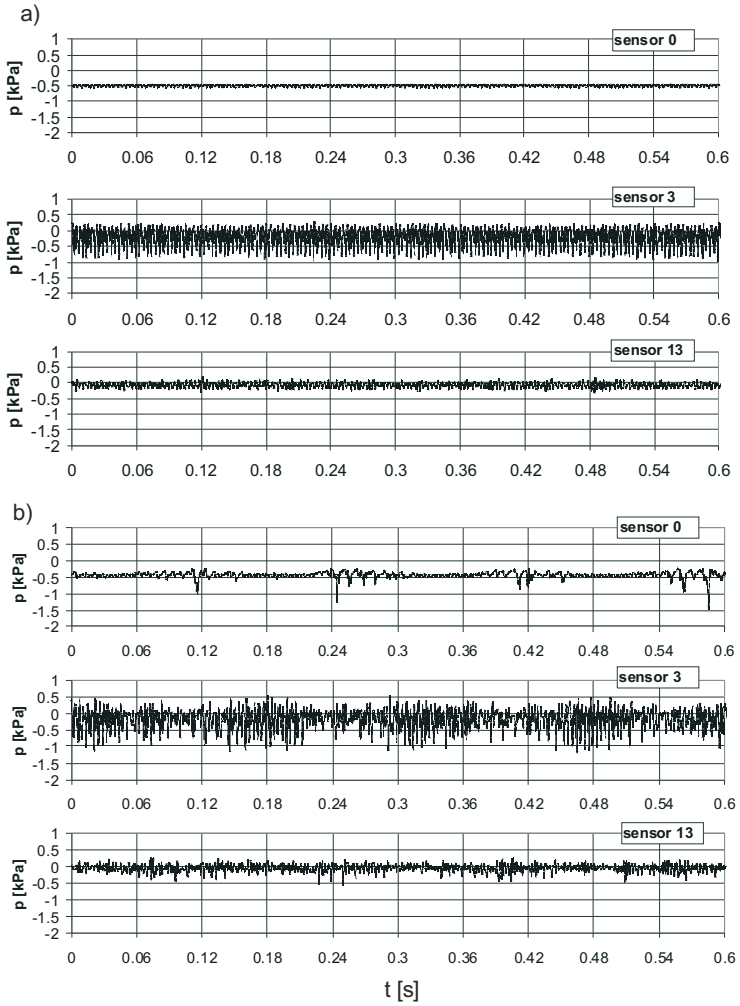

Fig. 7. Pressure fluctuations at axial locations at the nominal ϕ = 0,397 (a), and unsteady ϕ = 0,314 (b) point of operation

Fig. 7a. These figures show the wall static pressure signals at point "0" in the stalled, and unstalled flow. The most significant pressure oscillations at the stable point of operation are at the blade passing frequency. The amplitudes of pressure oscillations increased significantly in the cross-sections of the rotor blades with higher aerodynamic load (sensor 3 in Fig. 7a). A single stall cell is observed in fully developed stall conditions (Fig. 7b). In this region, the casing wall pressure is characterized by high fluctuation across the flow passage, what could be clearly seen near the leading edge of the rotor blades. Figures 7a,b confirm the significant effect of the flow in the tip region of the leading edge of the rotor on the flow stability. The high frequency of pressure oscillations during rotating stall is smaller than that of rotor rotation and significantly smaller than that of the blade passing frequency.

4.2. Investigations of the pressure fluctuations upstream of the rotor blades

A rotating stall is an unstable operating regime that can be induced in a compressor rotor by throttling the exit flow. Subsequent opening of the exit flow draws the compressor back to stable operation. This event, as sensed by a wall static pressure probe located at the measuring point "0" (Fig. 3b), is shown in Figs 8a,b. Three distinct phases of the rotating stall regime can be identified, as indicated in the picture: stall inception, developed stall, and stall recovery. Figure 8 shows also the phenomenon of the aerodynamic hysteresis loop. The stall inception occurs at a lower flow rate (ϕ=0.324) than the stall recovery (ϕ=0.331). The stable phase of the rotating stall regime occurs in the flow range: ϕ=0.314÷0.285. The next figure 9 shows the influence of the point of operation on the wall static pressure signals in the stable operation and during an established, rotating stall, and Fig. 10 shows amplitude spectra of these time functions.

As shown in the wall static pressure, and in its spectrum at ϕ=0.397 in Figure 9a and 10a, respectively, the influence of the blade passing dominates flow characteristics in the stable operating range. The stall flow region is indicated as "S" at ϕ=0.316 and 0.314, as shown in Figs 9 a, b, c. However, the unstalled flow region, indicated as "U", shows a similar pressure pattern with the stable operating range at ϕ=0.397. Inspection of data plotted in Fig.10, and the steadiness of the rotating stall period at different points of operation, indicate that there are single zones of rotating stall, with an averaged frequency decreased from $f_{r.s.}$=6.9 Hz at ϕ=0.316 to $f_{r.s.}$=5.9 at ϕ=0.285. The rotor shaft frequency was f_{SH}=16.66 Hz. The ratio of rotating stall and shaft frequencies changed in accordance to flow rate from 0.41 to 0.35. If the flow rate was reduced further to =0.285 (Fig. 9), the characteristic of the whole signal changed to the type of a non-periodic random signal,

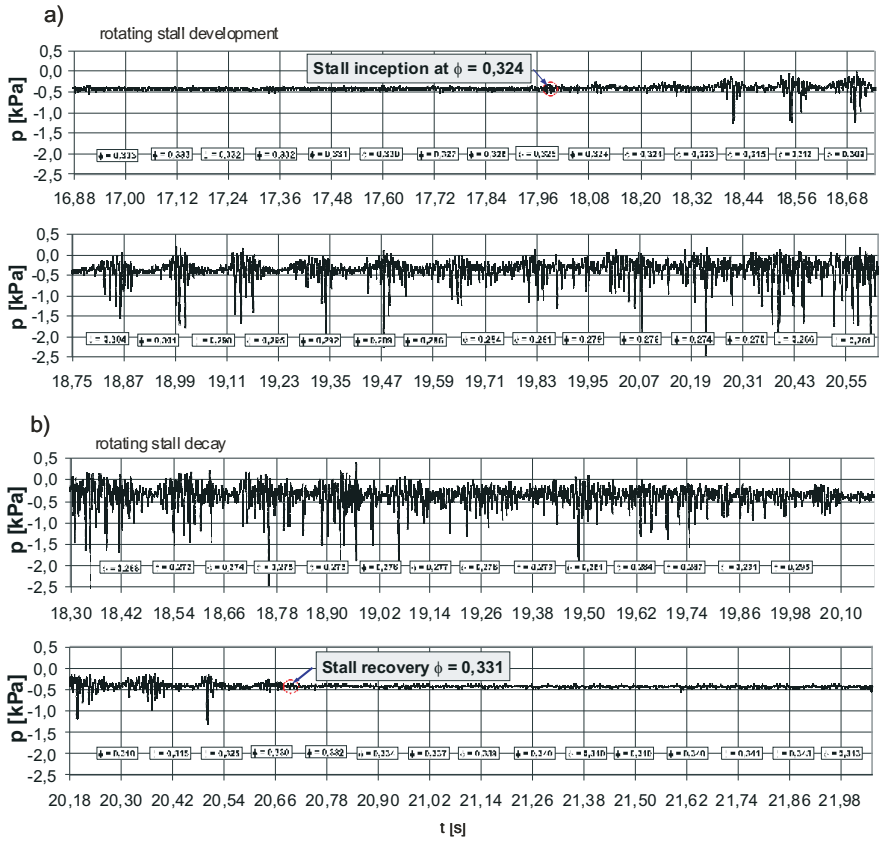

Fig. 8. Stalling pattern of research compressor stage during the throttling and opening of the exit throttle

contrary to what was observed at ϕ=0.397 and ϕ=0.316, and the random signal had a broadband frequency spectrum.

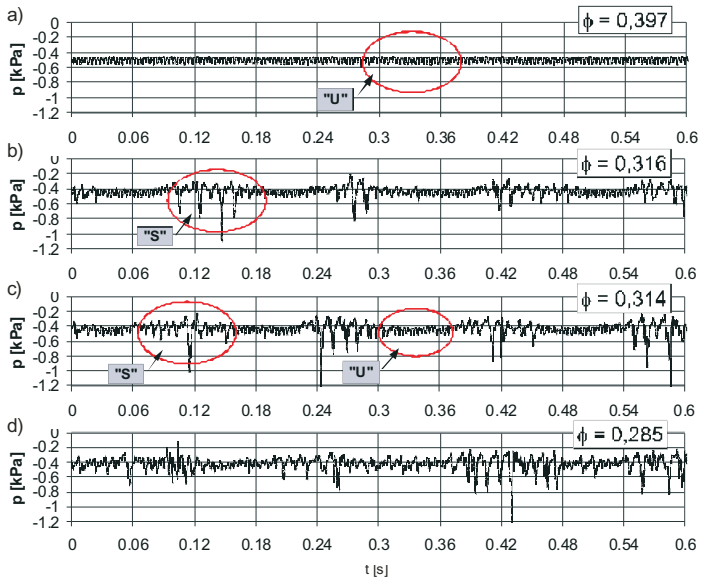

Fig. 9. Pressure signals upstream of the rotor at stable operating point and during stabilized rotating stall

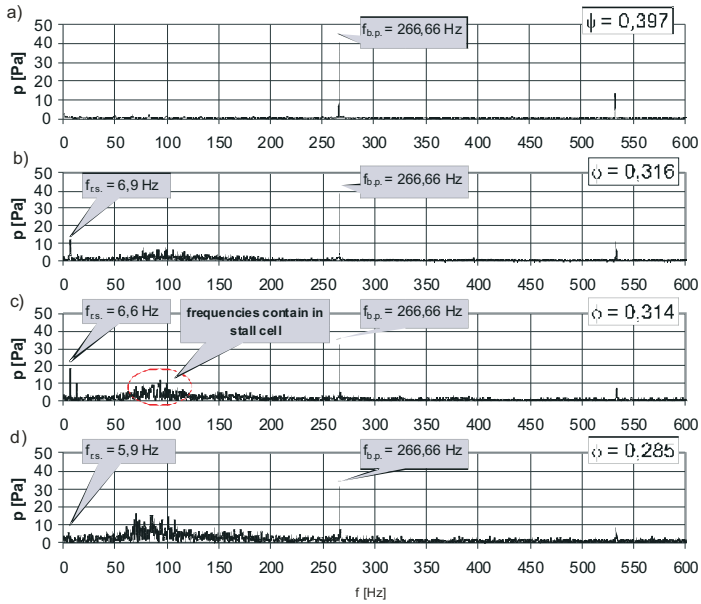

Fig. 10. Pressure amplitude spectra

4.3. The influence of operating point on circumferential extension of stall cell

The number of rotor blade-to-blade channels disturbed by the rotating stall at different points of operation is not the main subject of most papers. To examine the influence of point of operation on the spread of the stall cell in circumferential direction, we show in Figure 11 the instantaneous pressure fluctuations upstream of the rotor at different points of operation during an established process of rotating stall. We can see that at the flow rate ϕ=0.316 the number of rotor blade passages disturbed by the stall cell is equal to 50%. As the flow decreases to the value of ϕ=0.285, the disturbed region increases and occupies about 72% rotor-blade passages. These facts suggests that, when the flow-rate coefficient decreases from 0.316 to 0.285, the number of overloading blades with increased incidence and separated flow continuously increases.

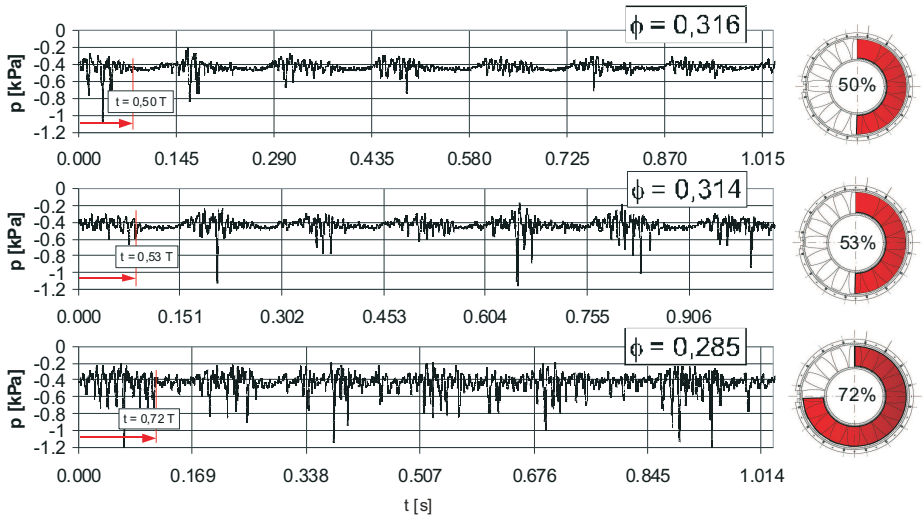

Fig. 11. Extension of the stall cell in the circumference of the rotor at the different points of operation

4.4. Investigations of pressure fluctuations in circumferential direction

To determine the number of stall cells, sixteen pressure sensors were placed around the circumference of the casing at the inlet of the rotor (Fig.3). The accuracy of this characteristic would increase with the increasing number of sensors. Fig. 12 shows pressure fluctuations over the circumference of the tip of the rotor in the transverse cross section “0” captured by five chosen pressure transducers, A through I, during the stabilized process of

stall rotation. The distance between the locations of the two sensors, A and I, is equal to 180°. The dashed lines in Fig.12 connects points at which the signals have the same phases of the rotor blade (RB) and cells rotation (CR). The phase differences between the oscillations recorded by any pair of the sensors are equal to the differences between the sensor locations on the rotor casing. The rotational period of the pressure field is equal to the period of pressure oscillation. From Fig.12, we may also find that the duration of the stall cell is equal to the time interval in which the blade rotates from the measuring point A to the point I. It confirms earlier observation that the pressure fluctuation represents the oscillation of one-stall cell which affects the flow at a flow rate of ϕ=0.314 around about 50% of the rotor blade channels. It is denoted by the dashed line marked with (CR).

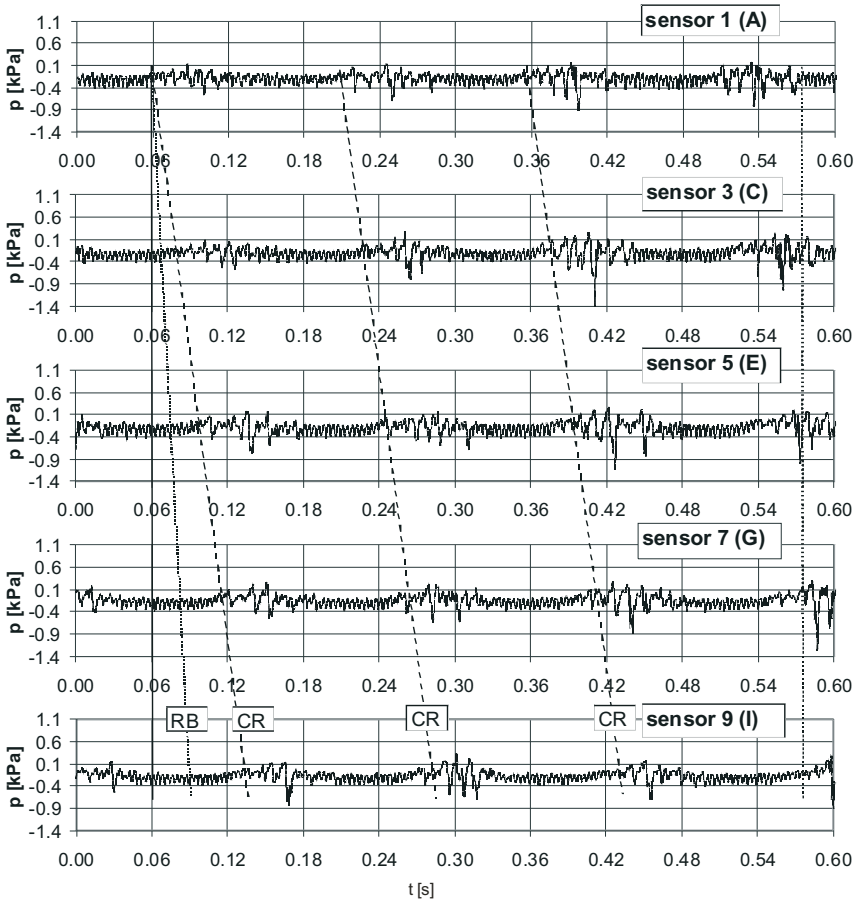

Fig. 12. Pressure variation over the circumference of the tip of the rotor at the point of operation at ϕ=0.314

4.5. Pressure contours at the rotor blade-to blade channels

In addition to the above phase-locked patterns, the pressure contour map are also discussed to facilitate better understanding of the unsteady flow phenomena. Figures 13a,b,c,d show phase-locked contour plots of the wall pressure at the rotor blade-to-blade channels, measured by pressure transducers placed along the rotor blade passage, as shown in Fig. 3b. The pressure contour plots were determined at the design point of operation (Fig.13a) and compared with those at the near stall inception (Fig.13b), and at the points of the stabilized process of stall rotation (Figs 13c,d) respectively. As shown in Fig.14a, the flow fields can be clearly divided into two regions: the region of leakage flow on the suction side and the incoming through flow region on the pressure side of the blade. The leakage flow region grows rapidly near the leading edge and increases gradually in the downstream of the blade channel.

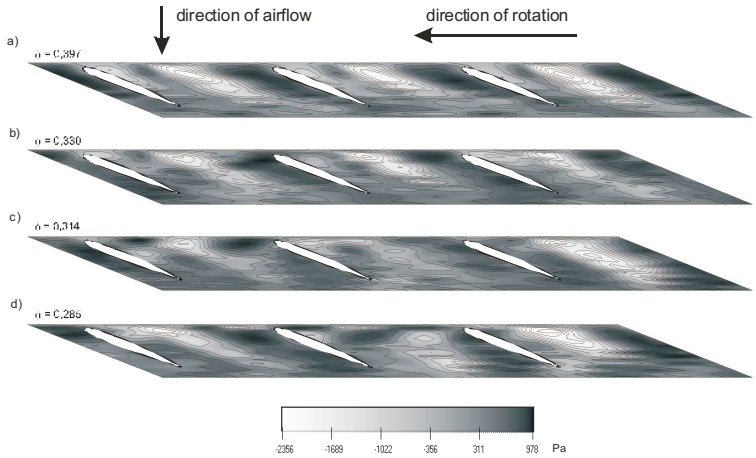

Fig. 13. Pressure contours at casing wall at different points of operation

This is due to the strong jet flow in the direction opposite to rotation caused by the large pressure difference between the pressure side and the suction side of the blades near the leading edge. It causes that the pressure between the pressure side and the suction side of he blade becomes even. Some additional disturbances are introduced by the blade wake and they appear in the area between the blade and departing clearance vortex. Figure 13 shows that the steady flow is the dominating one in the end-wall region in the cases when the flow rate equals 0.397 and 0.33. In addition to the potential flow field, the roll-up and trajectory of the tip clearance vortex can clearly be seen. Leakage vortex forms the low-pressure trough near the leading edge of the suction side. At the design flow rate, the low-pressure trough lies parallel to the suction side of the blade passage from the low-pressure core. As the

flow rate decreases, the low-pressure core shifts slightly toward the leading edge, and swings upstream toward the circumferential direction (Fig. 13b). Near the stall (Fig. 13c), the pressure trough becomes more perpendicular to the axial direction and directed against the leading edge of the subsequent blade. During the transition into the fully developed stall, the low pressure trough at some blade to blade channels disappears. It seems to be the result of the stall cell disturbances. Similar results were reported by others authors (e.g. INOUE et al. [1]). We can also see that, under normal flow condition, the phase-locked pattern has a periodic structure, with the period equal to the blade spacing, but the periodicity quickly disappears near the stall inception, as shown in Figs. 13c and 13d. As the flow rate decreases to ϕ=0.314 and ϕ=0285, one can observe a highly unsteady flow. The pressure contour maps have a variable intensity that changes from blade to blade. In order to find the blade to blade channels in which the stall cell occurs, we evaluated the contour plot maps in Fig 14 depicting the pressure distribution around the whole circumference of the rotor at a flow rate of ϕ=0.314 and for a selected single revolution of the rotor . It can be seen that, when the rotating stall appears, it causes that the pressure differences between the blades disappear in about 50% of the rotor channels. It could result from separation (S) and blockage (B) of the flow in these channels. It confirms earlier observations formulated in previous sections of this paper (see Fig.11).

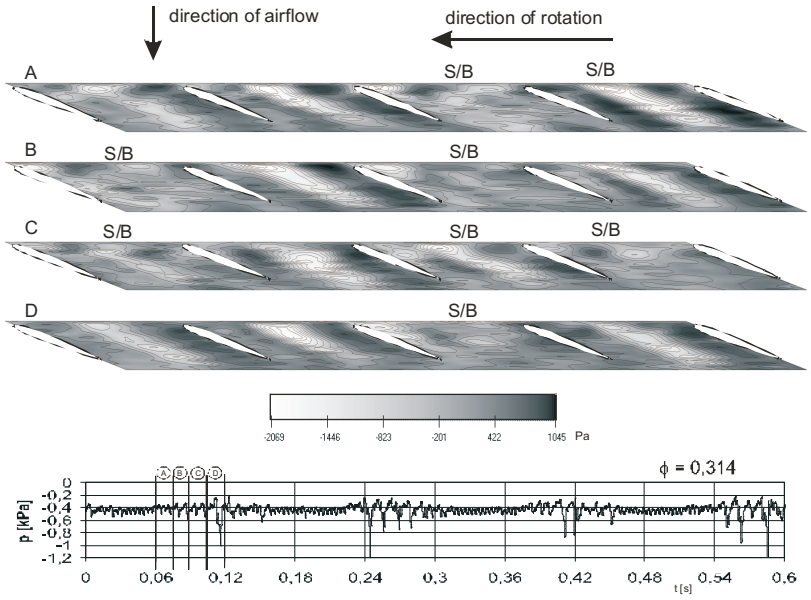

Fig. 14. Contour plots map of the pressure distribution in the whole circumferential extension of the rotor /16 channels/

5. Conclusions

The stall inception patterns, and the features of the stall cell in a low-speed axial-flow compressor stage were investigated experimentally by measurements of pressure and velocity fluctuations. The measurements of wall static pressure fluctuations, either at inlet of the rotor blade in the circumferential direction, or along the rotor blade passage, were performed in the stable and unstable points of operation. The first task of this study was to define the stall cell (stall zone) by pressure field analysis. Next, the nature of pressure fluctuation on the rotor casing wall was investigated to find a rotating stall precursor and the number of stall cells and their rotational speed at the different points of operation. The results can be summed up as follows:

1. The contour plots of the energy defect and turbulence intensity downstream of the rotor blade, at stable and unstable points of operation, allow us to conclude that the flow in the tip region of the compressor rotor has a significant effect on the compressor instability and stall inception.
2. Rotating instability is most clearly observed within the upstream region of the rotor blades.
3. The pressure signals appearing during the stabilized stall contain low-frequency pressure oscillations of the rotating stall, high-frequency pressure oscillations with frequency equal to the blade-passing frequency (BPF), and high-frequency oscillations in the frequency range between the rotor speed and the BPF.
4. In this paper, the authors have focused their attention on the relationship between the flow rate and stall cell oscillations and spread of the stall cell over the rotor circumference. A single stall cell was observed in fully developed stall conditions. When the flow rate was reduced, the ratio of frequencies of the rotating stall and the shaft decreased from 0.41 at flow rate of 0.316 to 0.35 at flow rate of 0.285. At the same time, the number of the rotor blade passages that are disturbed by the stall cell increased from 50% to 72%. This suggests that, when the flow-rate coefficient decreases from 0.316 to 0.285, the number of overloaded blades with increased incidence and separated flow continuously increases. These results suggests that the rotating stall pattern significantly depends on the point of operation which influences blade loading and flow separation.

Manuscript received by Editorial Board, April 07, 2008;
final version, November 21, 2008.

REFERENCES

[1] Inoue M., Kuroumaru M., Iwamoto T., Ando Y.: Detection of a rotating stall precursor in isolated axial flow compressor rotors. Journal of Turbomachinery, vol. 113, April 1991, pp.281-289.
[2] Nobuyuki T., Masahiro K., Yutaka O., Eisuke O., Tomofumi N., Yuki T.: Early stall warning technique for axial flow compressors. ASME Paper GT2004-53292.
[3] Day I. J.: Stall inception in axial flow compressors. ASME J. of Turbomachinery, 115, 1993, pp. 1-9.
[4] Inoue M, Kuroumaru M., Yoshida S., Furukawa M.: Short and length-scale disturbances leading to rotating stall in an axial compressor stage with different stator/rotor gaps. Trans. of the ASME , vol. 124, July 2002, pp 376-384.
[5] Maerz J., Hah C., Neise W.: An experimental and numerical investigation into the mechanisms of rotating instability. ASME J. of Turbomachinery, 2002, 124, pp. 367-375.
[6] Kim K. H., Shin Y. H., Kang C. S.: The measurements of unsteady flow field in an axial flow fan under stalled condition. Proc. of the International Gas Turbine Congress 2003 Tokyo, pp 1-5.
[7] Nishioka T., Kuroda S., Kozu T.: Influence of Rotor Stagger Rotating Stall inception in an Axial-flow Fan. Proc. of ASME Turbo Expo 2003, June 16-19, 2003, Atlanta.
[8] Levy Y., Pismenny J.: The number and speed of stall cells during rotating stall. Proc. of ASME Turbo Expo 2003, June 16-19, 2003, Atlanta.
[9] Levy Y., Pismenny J., Schrapp H., Stark U., Saathoff H.: Pressure field at the tip of rotor blades before and during rotating stall. Proc. of the 7th European Conference on turbomachinery Fluid Dynamics and Thermodynamics, 5-9 March 2007, Athens, Greece.
[10] Lepicovsky J., Braunscheidel E. P.: Measurement of flow pattern within a rotating stall cell in an axial compressor. NASA/TM-2006-214270, June 2006.
[11] Witkowski A., Majkut M.: Experimental investigation if inlet guide vane-rotor interaction in a low speed axial flow compressor stage. The Archives of Mechanical Engineering, Number 1, 2006.
[12] Witkowski A., Strozik M., Majkut M., Żukowski J.: Comprehensive Computational and Experimenal Methods of Investigations of the Unsteady Flow in an Axial Flow Low Speed Compressor Stage. 1-th edn. The Silesian University of Technology, Gliwice, 2007, pp 1-212.
[13] Witkowski A., Chmielniak T., Strozik M., Mirski M.: Facility for turbulence and unsteadiness measurements behind an axial compressor rotor blade by means periodic multisampling with triple split fiber probes. Proc. of the Second Biennial European Joint Conference on Engineering System Design and Analysis, London, July 4-7, 1994

Badania eksperymentalne zjawisk przepływowych w kanałach łopatkowych wirnika osiowego niskoobrotowego stopnia sprężającego w niestatecznym obszarze charakterystyki pracy

Streszczenie

W pracy przedstawiono eksperymentalne badania pulsacji ciśnienia w obszarze szczeliny nadłopatkowej łopatek koła wirnikowego, w osiowym, niskoobrotowym stopniu sprężającym, w statecznym i niestatecznym obszarze charakterystyki aerodynamicznej. Nieustalone impulsy ciśnienia próbkowane były za pomocą wysokoczęstotliwościowych przetworników ciśnienia zamontowanych na osłonie zewnętrznej koła wirnikowego. Przeanalizowano impulsy ciśnieniowe oraz ich charakterystyki częstotliwościowe zarówno w obszarze statecznej pracy koła wirniko-

wego, w obszarze przejścia, jak i w obszarze ustabilizowanego zjawiska niskoczęstotliwościowego oderwania wirującego. W miarę jak punkt pracy przemieszcza się do obszaru niestatecznej części charakterystyki pojawia się oderwanie wirujące z częstotliwością wynoszącą 41.4% częstotliwości obrotów wirnika. W wyniku przeprowadzonych badań stwierdzono, że w bada- nym niskoobrotowym stopniu sprężającym, występuje w kanałach międzyłopatkowych koła wirnikowego, jedna komórka oderwania, która obejmuje swym zasięgiem kilka sąsiednich kanałów. Dalsze zmniejszanie strumienia przepływu powoduje spadek częstotliwości wirującego oderwania do 34.8% częstotliwości obrotów wirnika oraz wzrost liczby kanałów łopatkowych, w których to oderwanie występuje.